Depth invariant index of the bottom type

Passive remote sensing techniques for mapping water depth and bottom features

David R. Lyzenga

Ratio processing methods are reviewed, and a new method is proposed for extracting water depth and bottom type information from passive multispectral scanner data. Limitations of each technique are discussed, and an error analysis is performed using an analytical model for the radiance over shallow water.

Introduction

Aerial photography of shallow water areas can provide useful qualitative information on bottom composition, the distribution of benthic algal or coral communities, and water depth. However, the interpretation of this photography is impeded by the fact that water depth variations are not easily distinguished from bottom color differences. Surface reflection effects add another element of confusion to the interpretation of the photography. The use of digitally recorded multispectral scanner data permits corrections to be made for surface reflection effects and also allows the possibility of automatic recognition of bottom features and water depth using radiometric techniques. Past research efforts have resulted in the development of specific techniques for each of these applications.[1,2] The purpose of this paper is to discuss the limitations of these techniques and to present a more general set of algorithms for both applications.

Ratio Algorithms

The techniques described in Refs. 1 and 2 were developed on the basis of a simple water reflectance model which accounts for the major part of the signal received by a multispectral scanner over clear shallow water, but neglects the effects due to scattering in the water and internal reflection at the water surface. According to this model, the radiance in a given wavelength band (i) can be written as

$$L_i = L_{si} + k_i r_{Bi} \exp(-\kappa_i f z), \tag{1}$$

where L_{si} is the radiance observed over deep water (due to external reflection from the water surface and scattering in the atmosphere); k_i is a constant which includes the solar irradiance, the transmittance of the atmosphere and the water surface, and the reduction of the radiance due to refraction at the water surface; r_{Bi} is the bottom reflectance; κ_i is the effective attenuation coefficient of the water; f is a geometric factor to account for the pathlength through the water; and z is the water depth.

The simplest method of extracting water depth information from multispectral scanner data is to invert Eq. (1) for a single wavelength band. An extension of this method would be to calculate the depth from two or more bands and average the results. The difficulty with this technique is, of course, that changes in the bottom reflectance or water attenuation cause errors in the depth calculation.

The water depth algorithm developed by Polcyn *et al.*[1] relies on the assumption that a pair of wavelength bands can be found such that the ratio of the bottom reflectances in these two bands is the same for all the bottom types within a given scene. That is, for bottom types $A, B, \ldots$,

$$\frac{r_{A1}}{r_{A2}} = \frac{r_{B1}}{r_{B2}} = \ldots = R_b, \tag{2}$$

where r_{A1} is the reflectance for bottom type A in band 1 etc. The water depth can then be calculated from the equation

$$z = \frac{1}{(\kappa_1 - \kappa_2) f}\left[\ln\left(\frac{k_1}{k_2}\right) - \ln\left(\frac{R}{R_b}\right)\right], \tag{3}$$

where R is the ratio of the bottom-reflected signals in the two bands:

$$R = (L_1 - L_{s1})/(L_2 - L_{s2}). \tag{4}$$

If the assumption expressed by Eq. (2) is correct, the depth calculated by this method is not affected by changes in bottom composition in the scene. The depth is also insensitive to changes in water quality if the

The author is with Environmental Research Institute of Michigan, P.O. Box 618, Ann Arbor, Michigan 48107.

Received 8 June 1977.
0003-6935/78/0201-0379$0.50/0.

difference between the attenuation coefficients ($\kappa_1 - \kappa_2$) remains constant. In many cases a pair of wavelengths can be found for which Eq. (2) is approximately satisfied, or for which ($\kappa_1 - \kappa_2$) remains relatively constant. However, the wavelengths which satisfy one criterion are in general not the same as those which satisfy the other, and if changes in bottom composition or water quality are too large, a pair of wavelengths may not exist which satisfies either criterion. Nevertheless, this method has been used with some success for extracting water depths from both satellite and aircraft multispectral scanner data over relatively clear water to a depth of approximately one attenuation length.[3,4]

The inverse problem is to extract information about the bottom reflectance (or bottom composition) from the radiance measured by the multispectral scanner. An algorithm was developed for this purpose[2] by noting that the radiance ratio R should be independent of the water depth if the effective water attenuation coefficients are the same in both bands. From the simple water reflectance model described above, this ratio then reduces to

$$R = (k_1 r_{B1})/(k_2 r_{B2}), \tag{5}$$

which may be used as an index of the bottom type, provided that the bottom types to be mapped have different reflectance ratios in the wavelength bands selected.

This method was successfully used for mapping the distribution of *Cladophora* (a green benthic algae) under a variable depth of water along the Lake Ontario shoreline.[2] The primary reason for the success of this application was the fact that the vegetation reflectance has distinctive features (due to chlorophyll absorption) in the blue–green region of the spectrum where the water attenuation is at a minimum. Thus it was possible to choose two bands with equal water attenuation coefficients and different bottom reflectance ratios for the green vegetation and the sand background.

In attempting to apply this method to a larger number of water types and bottom materials, however, several difficulties arose. First, the requirement of equal water attenuation coefficients in the operating wavelength bands causes operational difficulties, since the band positions must be changed when operating in different water types. Second, the requirement of different bottom reflectance ratios restricts the number of bottom materials that can be recognized, since materials with similarly shaped reflectance spectra (such as sand and mud) have nearly equal reflectance ratios. Finally, both ratio methods for bottom features and water depth are inherently restricted to two operating wavelength bands. Since independent information relating to both water depth and bottom composition can be collected simultaneously in several wavelength bands, methods which use only two of these bands do not make full use of the available information.

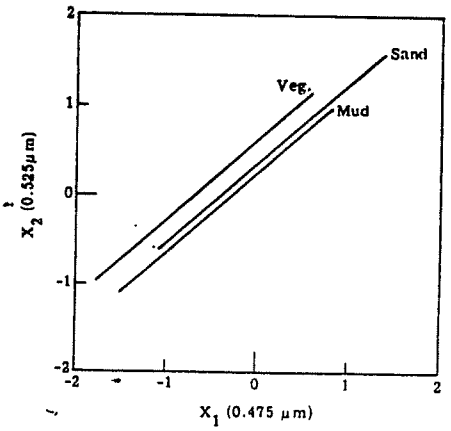

Fig. 1. Plot of X_1 vs X_2 for water type 3 with three bottom types. Water depth ranges from 0 m to 5 m on each curve.

More General Algorithms

In order to develop a more general set of algorithms for water depth and bottom features, the simple radiance model described above was modified to include the effects of scattering in the water and internal reflection at the water surface (see Appendix A). Examination of this model shows that the scattering term has the same depth dependence as the bottom-reflected radiance. Except for the effects of internal reflection, therefore, the total radiance for the case of direct incident radiation may be written in the same form as Eq. (1), with the actual bottom reflectance replaced by an apparent bottom reflectance

$$r_B' = r_B - \frac{\pi\beta(\mu_s)}{K(\mu + \mu')}. \tag{6}$$

The variables on the right-hand side of this equation are defined in Appendix A. This exponential depth dependence suggests the use of the transformation

$$X_i = \ln(L_i - L_{si}), \tag{7}$$

where L_{si} is the deep-water radiance (including scattering). The purpose of this transformation is to linearize approximately the relationship between the transformed radiances and the water depth. The nonlinearities which remain are caused by internal reflection effects, which are significant only for very shallow water and high bottom reflectances.

A plot of the transformed radiances over three bottom types at wavelengths of 0.475 μm and 0.525 μm is shown in Fig. 1. The water parameters used in this example are a composite of Jerlov's[5] irradiance attenuation coefficients for coastal water type 3 and Petzold's[6] scattering parameters for Station 5 off the coast of southern California. The irradiance attenuation coefficients were 0.223 m^{-1} and 0.198 m^{-1}, and the total scattering coefficient was 0.275 m^{-1} at the wavelengths used. In the absence of reliable reflectance measurements for actual bottom materials, the reflectances of beach sand, dark soil (representing mud), and wheat leaves (representing aquatic vegetation) were used for this calculation. These reflectances are plotted in Fig.

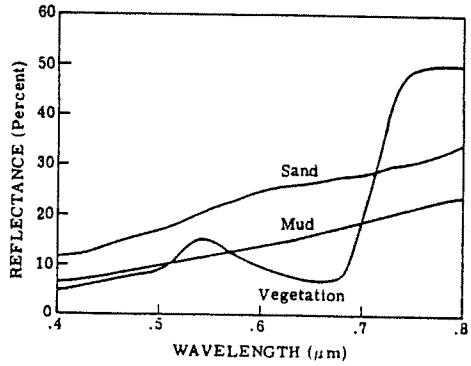

Fig. 2. Spectral reflectances of sand, mud, and green vegetation.

2. For these water and bottom parameters, the radiance due to scattering is equal to the bottom-reflected radiance at a depth of about 6 m.

Figure 1 represents a simulated data set for an ideal measurement situation with no noise and no variation in water or bottom parameters. For an actual data set, the data points would be randomly distributed about the lines in Fig. 1. Except for the slight curvature caused by internal reflection effects, the transformed radiance values over different bottom types describe parallel lines in X_i-space as the water depth varies continuously.

For an N-band system, the transformed radiances fall along a set of parallel lines in N-space. Thus, a second set of variables

$$Y_i = \sum_{j=1}^{N} A_{ij} X_j \tag{8}$$

can be obtained by rotating the coordinate system so that the Y_N axis is parallel to this direction (see Appendix B). If the linear transformation (8) is a pure rotation, only Y_N will be dependent on the water depth, while all the other variables are functions only of the bottom reflectance. For an N-band system, this results in a set of $N-1$ depth-invariant signals which can be used as inputs to a conventional maximum likelihood classification algorithm. The remaining variable can be written as

$$Y_N = B_m - Cz, \tag{9}$$

where B_m is a function of the bottom composition and C depends only on the water attenuation coefficients. If the bottom material can be recognized by the procedure outlined above, and the value of B_m determined for each bottom type, Eq. (9) can then be used to calculate the water depth.

Although this analysis bears a superficial resemblance to principal component analysis,[7] the only actual similarity is the use of a rotation transformation. In the case of principal component analysis, the first coordinate axis is aligned in the direction of maximum sample variance, and the remaining axes are aligned in the orthogonal directions with decreasing sample variance. The purpose of the principal component analysis as applied to water color[8] is to reduce the number of variables, since only a few of the principal components are usually needed to account for most of the sample variance. In the analysis presented here, the directions of the transformed coordinate axes are not necessarily related to the sample variance, and the purpose of the analysis is not to reduce the number of variables but to remove the depth dependence from all but one variable.

For a two-band system, the decision rule for bottom classification reduces to a simple test on the value of Y_1. That is, the bottom is classified as material m if

$$Y_{m1} < Y_1 < Y_{m2}, \tag{10}$$

where Y_{m1} and Y_{m2} are the lower and upper decision boundaries, respectively, for material m. If the radiances over a given bottom type m are assumed to be normally distributed (due to system noise) with mean value $\bar{L}_{im}$ and standard deviation $(NE\Delta L)_i$ in band i, the probability that this material will be classified as material n is approximately

$$P(m,n) = \tfrac{1}{2}\,\mathrm{erf}\left(\frac{d_1}{\sqrt{2}}\right) - \tfrac{1}{2}\,\mathrm{erf}\left(\frac{d_2}{\sqrt{2}}\right), \tag{11}$$

where

$$d_1 = (\bar{Y}_m - Y_{n1})/\sigma_m, \tag{12}$$

$$d_2 = (\bar{Y}_m - Y_{n2})/\sigma_m, \tag{13}$$

$$\sigma_m^2 = \sum_{i=1}^{2} A_{1i}^2 (NE\Delta L_i)^2/(\bar{L}_i - L_{si})^2. \tag{14}$$

The total probability of misclassification for material m is

$$\bar{P}(m) = 1 - P(m,m). \tag{15}$$

The total probabilities of misclassification for the three materials in Fig. 1 are plotted vs depth in Fig. 3 for $NE\Delta L = 0.05$ mW cm^{-2} sr^{-1} μm^{-1}.

It can be shown that for the case of two bands with equal attenuation coefficients, the method described above is equivalent to the ratio method. However, in this case the performance of both methods is worse than that shown in Fig. 3 because of the similar reflectance

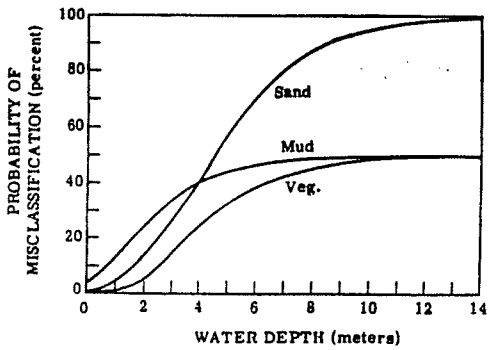

Fig. 3. Total probability of misclassification for three bottom types in water type 3, using the proposed method.

ratios of sand and mud. Thus, the performance of the ratio method can always be equaled and can usually be exceeded by the use of the proposed method with a more optimum pair of wavelengths. Further improvement in bottom classification would be expected if more than two bands were used.

After the bottom classification has been performed, the water depth can be calculated from Eq. (9), using the appropriate value of B_m for material m. Depth errors arise from the variance of Y_N due to noise, which is approximately given by

$$(\Delta Y_N)^2 = \sum_{i=1}^{N} A_{Ni}^2 (NE\Delta L_i)^2/(L_i - L_{si})^2 \qquad (16)$$

and from errors in bottom classification. Thus the total rms depth error for bottom type m is

$$\Delta Z_m = \frac{1}{C}\left[(\Delta Y_N)^2 + \sum_n P(m,n)(B_m - B_n)^2\right]^{1/2}. \qquad (17)$$

The average depth error for the three bottom types in water type 3 is plotted vs depth in Fig. 4. For comparison, the depth error due to noise only using the ratio method is also plotted in Fig. 4. The rms depth error due to noise for the ratio method is given by

$$\Delta Z_r = \frac{1}{(\kappa_1 - \kappa_2)f}\left[\left(\frac{NE\Delta L_1}{L_1 - L_{s1}}\right)^2 + \left(\frac{NE\Delta L_2}{L_2 - L_{s2}}\right)^2\right]^{1/2}. \qquad (18)$$

The depth error is in general minimized by choosing wavelength bands with the smallest attenuation. In the ratio method, however, the sensitivity to noise increases rapidly as the difference between the attenuation coefficients in the two bands decreases. Since this difference is only 0.025 m^{-1} in the above example, these are not the optimum wavelengths for the ratio method. For any choice of wavelengths, however, the depth error due to noise is larger for the ratio method than for the method described above. The ratio method is also subject to errors due to changes in bottom composition: although these can be reduced by an appropriate choice of wavelengths, they can never in practice be completely eliminated.

Conclusions

The ratio algorithms for water depth and bottom features mapping are relatively simple techniques which give acceptable results in many situations. However, these algorithms are limited by operational restrictions which reduce their applicability and utility. A more general algorithm has been defined, and a preliminary evaluation of this method has been performed using a simulation model for the water radiance.

The advantages of this method for mapping bottom features are (1) increased operational flexibility, in that the wavelength bands are not limited to those with equal water attenuation coefficients, (2) better discrimination of bottom materials with similarly shaped reflectance spectra, and (3) improved performance through the use of more than two wavelengths bands.

The advantages of this method for mapping water depth are (1) increased operational flexibility, since the wavelength bands are not restricted by the requirement of equal bottom reflectance ratios for all bottom types, (2) lower sensitivity to noise, and (3) improved performance through the use of more than two wavelength bands.

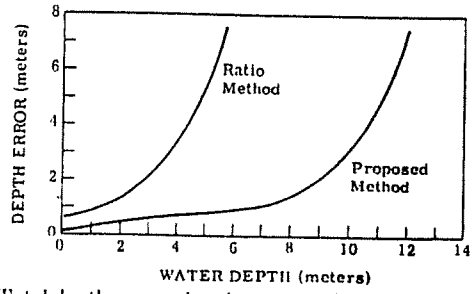

Fig. 4. Total depth error using the proposed method and depth error due to noise using the ratio method for water and bottom types shown in Fig. 1.

The disadvantage of the algorithm defined here is that it is more complex and therefore somewhat more difficult to implement than the ratio methods. The subtraction and division operations required for the ratio methods can be implemented by either analog or digital processors, whereas the method defined here requires digital computation. The input parameters for this algorithm are also somewhat more difficult to determine than those for the ratio methods.

Numerical results illustrating the performance of this method have been presented for one example situation. These results should not be considered as definitive of the best possible performance, since the wavelengths considered are not necessarily the optimum ones nor are the reflectances used necessarily representative of actual bottom types. In addition, better performance can be obtained by reducing system noise and by using more than two wavelength bands. The value of $NE\Delta L$ used in these calculations was 0.05 mW cm^{-2} sr^{-1} μm^{-1}. This is a typical value for an aircraft multispectral scanner with an angular field of view of a few milliradians, a spectral resolution of about 0.025 μm, and a collector area of about 80 cm^2. This noise equivalent radiance can readily be reduced by a factor of 2 or 3, with a corresponding reduction in the depth error, by increasing the collector area or reducing the spatial or spectral resolution of the system.

This work was supported by the Office of Naval Research, contract N000-14-74-C-0273.

Appendix A: Shallow-Water Radiance Model

The radiances shown in Fig. 1 were calculated using a combined water–atmosphere radiance model which includes the effects of scattering in the atmosphere and reflection at the water surface, as well as the components originating in the water itself. The atmospheric effects are calculated from the double-delta approximation,[9] using the atmospheric parameters tabulated by Elterman.[10] A solar zenith angle of 20° and a platform altitude of 1 km were used for the calculations in this report.

The water radiance is calculated using the quasi-single-scattering approximation,[11] modified to include the effects of reflection from the bottom[12] and internal reflection at the water surface.[13] The effects of internal reflection are included to all orders by assuming that the upwelling radiance distribution just beneath the water surface has a uniform angular distribution. Thus, the upwelling underwater radiance can be written as $L(\mu',\phi)$

$$= \frac{E_0'S(\mu',\mu_0',\phi) + \int_0^1 \int_0^{2\pi} L'(\mu'',\phi'')S(\mu',\mu'',\phi'')\mu''d\mu''d\phi''}{1 - \int_0^1 \int_0^{2\pi} R(\mu'')S(\mu',\mu'',\phi'')\mu''d\mu''d\phi''}, \quad \text{(A1)}$$

where E_0' is the direct solar irradiance penetrating the water surface, $L'(\mu'',\phi'')$ is the transmitted sky radiance below the surface, μ_0' is the cosine of the apparent solar zenith angle below the surface, $R(\mu'')$ is the Fresnel reflectance of the water surface, and

$$S(\mu,\mu',\phi) = \frac{1}{K}(\mu + \mu')^{-1}\left\{1 - \exp\left[-\left(\frac{1}{\mu} + \frac{1}{\mu'}\right)Kz\right]\right\}\beta(\mu_s) + \frac{r_B}{\pi}\exp\left[-\left(\frac{1}{\mu} + \frac{1}{\mu'}\right)Kz\right], \quad \text{(A2)}$$

where K is the irradiance attenuation coefficient,[14] z is the water depth, $\beta(\mu_s)$ is the volume scattering function, r_B is the bottom reflectance, and

$$\mu_s = -\mu\mu' + [(1-\mu^2)(1-\mu'^2)]^{1/2}\cos\phi. \quad \text{(A3)}$$

The results of this model agree with exact calculations using the Monte Carlo method[15] to within about 10% for values of the single-scattering albedo less than 0.8 and bottom reflectances less than 50%.

Appendix B: Coordinate System Rotation Parameters

The assumption involved in making the coordinate transformation (8) is that the variables X_i are linearly correlated with the water depth z, that is,

$$\hat{X}_i = a_i - b_i z \quad \text{(B1)}$$

with possibly different values of a_i for each bottom type. It is desired to transform this set of N depth-dependent variables into a new set of $N - 1$ depth-independent variables $(Y_1 \ldots Y_{N-1})$ and one depth-dependent variable (Y_N). The required transformation may be visualized as a pure rotation in N-space such that the Y_N axis is oriented in the direction specified by the parametric Eq. (B1). Thus, the transformation parameters for Y_N are

$$A_{Nj} = b_j\left(\sum_{k=1}^{N} b_k^2\right)^{-1/2}. \quad \text{(B2)}$$

The remaining parameters can be calculated using the conditions for the orthonormality of the new coordinate axes

$$\sum_{k=1}^{N} A_{ik}A_{jk} = \begin{cases} 0, & i \neq j \\ 1, & i = j \end{cases} \quad \text{(B3)}$$

and the condition for a proper rotation

$$\det(A_{ij}) = 1. \quad \text{(B4)}$$

These conditions uniquely define the transformation matrix only for the case $N = 2$. For three or more dimensions, however, a unique solution can be obtained by requiring that the coefficients for $Y_1 \ldots Y_{N-1}$ be the same for the $(N + 1)$-dimensional case as for the N-dimensional case. The coefficients for the $(N - 1)$ depth-independent variables are then

$$A_{ij} = b_{i+1}b_j\left(\sum_{k=1}^{i} b_k^2\right)^{-1/2}\left(\sum_{k=1}^{i+1} b_k^2\right)^{-1/2} \quad \text{for } j = 1 \ldots i, \quad \text{(B5)}$$

$$A_{ij} = -\left(\sum_{k=1}^{i} b_k^2\right)^{1/2}\left(\sum_{k=1}^{i+1} b_k^2\right)^{-1/2} \quad \text{for } j = i + 1, \quad \text{(B6)}$$

$$A_{ij} = 0 \quad \text{for } j = i + 2 \ldots N. \quad \text{(B7)}$$

These equations, along with Eq. (B2), completely define the required coordinate transformation. The values of b_i can be calculated if the water attenuation coefficients are known or can be empirically obtained from a regression analysis of the measured radiance values over a uniform bottom.

References

1. F. C. Polcyn, W. L. Brown, and I. J. Sattinger, "The Measurement of Water Depth by Remote Sensing Techniques," Report 8973-26-F, Willow Run Laboratories, The University of Michigan, Ann Arbor (1970).
2. C. T. Wezernak and D. R. Lyzenga, Remote Sensing Environ. 4, 37 (1975).
3. F. C. Polcyn and D. R. Lyzenga, "Calculation of Water Depth from ERTS—MSS Data," in *Proceedings Symposium on Significant Results Obtained from ERTS-1*, NASA Publication SP-327 (1973).
4. D. Lyzenga and F. Thomson, "Data Processing and Evaluation for Panama City Coastal Survey: Bathymetry Results," Report 121400-1-T, Environmental Research Institute of Michigan, Ann Arbor, Mich. (1976).
5. N. G. Jerlov, *Optical Oceanography* (Elsevier, New York, 1968).
6. T. J. Petzold, "Volume Scattering Functions for Selected Ocean Waters," Visibility Laboratory Tech. Report 72-78, Scripps Institution of Oceanography, San Diego, Calif. (1972).
7. J. L. Mueller, Appl. Opt. 15, 394 (1976).
8. W. R. McCluney, Remote Sensing Environ. 5, 3 (1976).
9. W. A. Malila, R. B. Crane, C. A. Omarzu, and R. E. Turner, Studies of Spectral Discrimination, Report 31650-22-T, Willow Run Laboratories, University of Michigan, Ann Arbor (1971).
10. L. Elterman, "UV, Visible and IR Attenuation for Altitudes to 50 km," Report AFCRL-68-0153, Air Force Cambridge Research Laboratories, Bedford, Mass. (1970).
11. H. R. Gordon, Appl. Opt. 12, 2803 (1973).
12. W. R. McCluney, "Estimation of Sunlight Penetration in the Sea for Remote Sensing," NASA Report TM X-70643 (1974).
13. D. R. Lyzenga, Appl. Opt. 16, 282 (1977).
14. The use of K instead of $c^* = (1 - w_0F)c$ in the quasi-single-scattering approximation represents a further approximation, which is valid if K is measured under direct solar illumination with the sun near zenith, see H. R. Gordon, J. Opt. Soc. Am. 64, 773 (1974).
15. H. R. Gordon and O. B. Brown, Appl. Opt. 13, 2153 (1974).